Biogeosciences Discuss., 5, 4001–4034, 2008
www.biogeosciences-discuss.net/5/4001/2008/

Biogeosciences Discussions

Biogeosciences Discussions is the access reviewed discussion forum of *Biogeosciences*

An empirical model simulating long-term diurnal CO_2 flux for diverse vegetation types

M. Saito[1], S. Maksyutov[1], R. Hirata[2], and A. D. Richardson[3]

[1]Center for Global Environmental Research, National Institute for Environmental Studies, Tsukuba 305-8506, Japan
[2]National Institute for Agro-Environmental Sciences, Tsukuba 305-8604, Japan
[3]Complex Systems Research Center, University of New Hampshire, Durham, NH 03824, USA

Received: 27 August 2008 – Accepted: 27 August 2008 – Published: 9 October 2008

Correspondence to: M. Saito (saito.makoto@nies.go.jp)

Published by Copernicus Publications on behalf of the European Geosciences Union.

Abstract

We present an empirical model for the estimation of diurnal variability in net ecosystem CO_2 exchange (NEE). The model is based on the use of a nonrectangular hyperbola for photosynthetic response of canopy and was constructed by using a dataset obtained from the AmeriFlux network and containing continuous eddy covariance CO_2 flux from 26 ecosystems over seven biomes. The model uses simplified empirical expression of seasonal variability in biome-specific physiological parameters with air temperature, vapor pressure deficit, and precipitation. The physiological parameters of maximum CO_2 uptake rate by the canopy and ecosystem respiration had biome-specific responses to environmental variables. The estimated physiological parameters had reasonable magnitudes and seasonal variation and gave reasonable timing of the beginning and end of the growing season over various biomes, but they were less satisfactory for disturbed grassland and savanna than for forests. Comparison with observational data revealed that the diurnal cycle of NEE was generally well predicted all year round by the model. The model gave satisfactory results even for tundra, which had very small amplitudes of NEE variability. These results suggest that this model with biome-specific parameters will be applicable to numerous terrestrial biomes, particularly forest ones.

1 Introduction

Atmospheric CO_2 variability simulation by atmospheric transport modeling depends critically on the use of terrestrial ecosystem models to accurately simulate diurnal and seasonal variations in terrestrial biospheric processes. Comparisons of seasonal cycles and their amplitude between the observed atmospheric CO_2 variability and that simulated by several terrestrial ecosystem models based on simplified assumptions of biospheric processes have often shown poor agreement (e.g., Nemry et al., 1999). However, Fung et al. (1987), for example, succeeded in adjusting the seasonal cycle amplitude by modifying the value of the Q_{10} temperature coefficient for ecosystem

BGD

5, 4001–4034, 2008

respiration.

Successful simulations of seasonal cycle phases have been made with more recent sophisticated models e.g., CASA (Potter et al., 1993; Randerson et al., 1997). Process based models differ in their parameterization of primary production. Models based on light-use efficiency, such as CASA and TURC (Ruimy et al., 1996), assume a linear relationship between monthly net primary production (NPP) and monthly solar radiation (Monteith, 1972), limited by water availability and temperature. Although these models appear to be successful in seasonal cycle simulation as a whole, their extension to cover diurnal cycles should be accompanied by the introduction of a more realistic, non-linear relationship between CO_2 uptake by terrestrial vegetation and solar radiation at an hourly time scale. The biochemical model proposed by Farquhar et al. (1980) describes the dependence of photosynthesis rate on solar radiation, with CO_2 uptake rate limited by maximum photosynthetic capacity. This concept is used widely in land-surface schemes for meteorology and hydrology, such as SiB (Sellers et al., 1986) and LSM (Bonan, 1996, 1998), but is less successful in carbon cycle studies because of a lack of empirical data or models for describing the seasonal and spatial variability of the necessary parameters, such as maximum photosynthetic capacity. Alternative ways of evaluating biospheric processes are required for the estimation of diurnal cycles in CO_2 variability, empirical models can fit the data more usefully than mechanistic models (Thornley, 2002).

For studies of the diurnal cycle of CO_2 variability, long-term field measurement studies by the eddy covariance method have also been conducted in recent years at many sites covering various ecosystems around the world (Baldocchi et al., 2001). These worldwide sites are now organized into a global network, FLUXNET, and a large body of the observed data is being accumulated. The eddy covariance method routinely provides direct measurements of net ecosystem CO_2 exchange (NEE) rate between the atmosphere and the biosphere. The eddy covariance method certainly has problems, including the narrow footprint of the representative spatial scale, nocturnal measurement, gap-filling methods and closure problems. Nevertheless, the data obtained from

BGD
5, 4001–4034, 2008

these field measurements can be useful, especially for constructing models to predict the diurnal cycle of CO_2 variability associated with biospheric processes, since they provide direct information on turbulence and scalar fluctuations at time scales from seconds to an hour over the local vegetation canopy.

We constructed an empirical model using extensive long-term eddy covariance CO_2 flux data to predict the diurnal variability in NEE over numerous ecosystems as simply as possible by empirical regression methods. We also characterized the seasonal variability in some physiological parameters with changes in environmental factors.

2 Materials and methods

2.1 Input data

All half-hourly or hourly CO_2 flux data used were obtained from the AmeriFlux network (Hargrove et al., 2003). Sixty-nine years' worth of eddy covariance flux data taken from 26 AmeriFlux ecosystem sites and covering seven major biomes in the latitudes from Alaska to Brazil were analyzed. The biomes consisted of six evergreen needle-leaf forests (ENF), two evergreen broad-leaf forests (EBF), four deciduous broad-leaf forests (DBF), four mixed forests (MF), five grasslands (GRS), two savannas (SVN), and three tundras (TND), (Table 1). Each site was equipped with an eddy covariance system consisting of an open- or closed-path infrared gas analyzer and a three-dimensional sonic anemometer/thermometer. Only measured fluxes, and not gap-filled values, were used to avoid the contamination associated with differences in gap-filling procedures. The periods analyzed for each ecosystem site are listed in Table 1.

Half-hourly or hourly air temperature (°C), vapor pressure deficit (VPD; kPa), incident photosynthetic photon flux density (PPFD; μmol photon m^{-2} s^{-1}), and precipitation (mm) for individual sites were also obtained from the AmeriFlux network. For all sites, air temperature and precipitation data that were missing because of instrument malfunction were filled by using Global Surface Summary of Day (GSOD) data sets to

BGD
5, 4001–4034, 2008

compute annual mean temperature and annual precipitation.

2.2 Modeling approach

To predict vegetation photosynthesis and its light response, a nonrectangular hyperbolic model:

$$\mathrm{NEE} = \frac{1}{2\theta}\left(\alpha Q + \beta - \sqrt{(\alpha Q + \beta)^2 - 4\alpha\beta\theta Q}\right) - \gamma \quad (1)$$

has been widely applied (e.g., Rabinowitch, 1951; Peat, 1970), where α is the initial slope of the light response curve and an approximation of the canopy light utilization efficiency (μmol CO_2 (μmol photon)$^{-1}$), β is the maximum CO_2 uptake rate of the canopy, known as P_{max} (μmol CO_2 m^{-2} s^{-1}), γ is the average daytime ecosystem respiration (μmol CO_2 m^{-2} s^{-1}), θ is a curvature parameter, and Q is PPFD. Johnson and Thornley (1984) have shown that the nonrectangular hyperbola predicts the integrated daily canopy photosynthesis with an accuracy better than 1% when it is averaged over various irradiances. More recently, this hyperbola has been successfully used in the gap-filling method to obtain continuous eddy covariance CO_2 fluxes over a year, and to estimate total annual carbon budget over various biomes (e.g., Gilmanov et al., 2003; Hirata et al., 2008).

Here, we derive a simple and empirical model for predicting the diurnal variability in NEE over a number of biomes on the basis of the nonrectangular hyperbolic model (e.g., Gilmanov et al., 2003). To apply the nonrectangular hyperbola, unknown number parameters (α, β, and γ in Eq. 1) have to be determined, whereas θ is fixed at 0.9 (e.g., Gutschick, 1991). To formulate individual unknown parameters we first calculated the seasonal course of those parameters for every site listed in Table 1 by using all available daytime data. The values of parameters were estimated for each day by fitting the data to Eq. (1) using the least-squares method. To reduce poor fitting of Eq. (1) resulting from the availability of only small numbers of available CO_2 flux data, the parameters for each day were estimated by using a 15-day period, which covers a period

of 7 days backward and 7 forward. Individual parameters exhibited seasonal variations, and the variability and amplitudes of individual parameters clearly differed among the ecosystem sites and biomes measured. Below we describe how we formulated the seasonal courses of three unknown parameters for each biome.

The seasonal course of P_{max} (β in Eq. 1) was correlated with those of temperature and VPD for each biome, and the strength of the correlations with these environmental factors differed among biomes. CO_2 assimilation rate also responds to other environmental factors, such as intercellular and external CO_2 concentrations at the leaf level (e.g., Leuning, 1990). However, in the interest of reducing the number of parameters and using meteorological data that were readily available everywhere, we defined P_{max} as a functions of temperature and VPD as follows:

$$P_{max} = P_{max}^{PM} \cdot F_T \cdot F_V \quad (2)$$

where P_{max}^{PM} is the potential maximum value of P_{max} under unstressed conditions, and F_T and F_V denote the coefficient functions for temperature and VPD, respectively. A bell-shaped curve (Raich et al., 1991; Ito and Oikawa, 2002) was adopted as F_T:

$$F_T = \frac{(T_a - T_{max})(T_a - T_{mim})}{(T_a - T_{max})(T_a - T_{mim}) - (T_a - T_{opt})^2} \quad (3)$$

where T_{max}, T_{min}, and T_{opt} are the maximum, minimum, and optimum temperatures (°C), respectively, for photosynthesis, as determined empirically for each biome (Table 2). T_a is the daily mean air temperature (°C) averaged over a 15-day period, consistent with that used in the fitting of Eq. (1). F_V is expressed as an exponential function:

$$F_V = \exp(a_{FV} \cdot (VPD_a - b_{FV})) \quad (4)$$

where a_{FV} and b_{FV} are constant coefficients empirically determined for each biome (Table 2), and VPD_a represents the daily mean value of VPD over a 15-day period, as used for T_a in Eq. (3).

BGD
5, 4001–4034, 2008

To formulate P_{max}^{PM} in Eq. (2), the yearly maximum value of P_{max} obtained by fitting of Eq. (1) with observed CO_2 flux data was selected for each site and then divided by F_T and F_V (see Eq. 2). To avoid uncertainty in the value of P_{max} due to random flux measurement error, a computed unstressed maximum P_{max} was averaged for the 7-day period around the maximum day. This value was defined as P_{max}^{PM}. Next, P_{max}^{PM} was approximated as a function of annual NPP, assuming that the maximum value of P_{max} was proportional to the annual NPP. Annual NPP (g C m^{-2} y^{-1}) for each site was estimated by using the Miami model (Lieth, 1975), as follows:

$$\mathrm{NPP}(\mathrm{AMT}, \mathrm{AP}) = \min\{\mathrm{NPP_T}(\mathrm{AMT}), \mathrm{NPP_h}(\mathrm{AP})\}; \quad (5)$$

$$\mathrm{NPP_T}(\mathrm{AMT}) = \frac{1350}{1 + \exp(1.315 - 0.119 \cdot \mathrm{AMT})},$$

$$\mathrm{NPP_h}(\mathrm{AP}) = 1350(1 - \exp(-0.000664 \cdot \mathrm{AP}))$$

where AMT is annual mean temperature (°C) and AP is annual precipitation (mm). The unstressed maximum P_{max} (i.e. P_{max}^{PM}) computed from the observed CO_2 flux data increased substantially with increasing NPP (Fig. 1). This P_{max}^{PM} dependence on NPP was found for all biomes we examined. P_{max}^{PM} was defined as follows:

$$P_{max}^{PM} = a_{PM} \exp(b_{PM} \cdot \mathrm{NPP}) \quad (6)$$

where a_{PM} and b_{PM} are constant coefficients empirically determined for each biome by the least-squares method (Table 2).

The initial slope α in Eq. (1) shows the complicated seasonal course of the light response curve and of P_{max}, as shown in previous studies (e.g., Gilmanov et al., 2003). Owen et al. (2007) have shown that the initial slope can be expressed as a linear function of canopy CO_2 uptake capacity. Similarly, we found that seasonal variation in the initial slope was correlated with that in P_{max} (Fig. 2). Therefore, we defined the initial slope α as a linear function of P_{max}:

$$\alpha = a_{Ini} \cdot P_{max} + b_{Ini} \quad (7)$$

where a_{lni} and b_{lni} are also constant coefficients empirically determined for each biome by the least-squares method (Table 2).

Ecosystem respiration (RE) (i.e. γ in Eq. 1) is the sum of autotrophic plant respiration and heterotrophic soil respiration. RE is usually expressed as a function of soil temperature (e.g., Falge et al., 2001). It has been further argued that RE varies with differences in short- and long-term temperature sensitivities (Reichstein et al., 2005), the start of the wet season and the timing of rain events (Xu and Baldocchi, 2004), differences in temperature sensitivities among ecosystem sites, even in the same biome (Gilmanov et al., 2007), and photosynthetic rate (Sampson et al., 2007). Accordingly, we can expect that seasonal variation in RE is in part site specific, so its universal attributes are difficult to formulate with a single equation. However, for application over large areas covering numerous biomes, a simple model driven by few input data is required. We therefore assumed that ecosystem loss by respiration has to be primarily in equilibrium with, or smaller than, ecosystem production by photosynthesis, although the relationship between NPP and RE may differ in the different stages of development in the course of a plant's life. Hence, the values of RE estimated by fitting of Eq. (1) by the least-squares method were scaled by annual NPP every years. Each was then bin-averaged over all periods for each site and related to temperature by using the exponential regression model (Lloyd and Taylor, 1994), as follows:

$$\frac{\mathrm{RE}}{\mathrm{NPP}} = \mathrm{RE}_{\mathrm{ref}} \exp\left[E_0\left(\frac{1}{T_{\mathrm{ref}} - T_0} - \frac{1}{T_{\mathrm{a}} - T_0}\right)\right] \quad (8)$$

where $\mathrm{RE}_{\mathrm{ref}}$ is the ecosystem respiration rate at the reference temperature T_{ref}, E_0 is a constant function, and T_0 is the lower temperature limit for ecosystem respiration, fixed at -46.02°C (Lloyd and Taylor, 1994; Reichstein et al., 2002). T_{ref} was set to 10°C. $\mathrm{RE}_{\mathrm{ref}}$ and E_0 were empirically determined for each biome by using the least-squares method (Table 2). Although there is a discrepancy in the units of time and matter between RE and NPP in Eq. (8), we used the original Miami model to simplify the model calculation. Figure 3 is an example of the temperature sensitivity of RE scaled by annual NPP

in savannas. RE/NPP increases systematically with increasing temperature; some degree of scatter is present.

To summarize the approach used for modeling diurnal variations in NEE presented in the section above, all parameters required to operate the model involve only four variables: temperature, VPD, annual precipitation, and PPFD. In applying the model, the parameters P_{max} and the initial slope in the nonrectangular hyperbola are estimated by using Eqs. (2) and (7) for each day, whereas the value of P_{max}^{PM} in Eq. (2) is determined for each year by using Eq. (6). Hence, diurnal variation in gross primary production (GPP – the first term on the right-hand side in Eq. (1) – is attributed to changes in the diurnal course of PPFD, as obtained from local observed data. On the other hand, RE is estimated for every half-hourly or hourly time step, both during the day and at night with local observed temperature data in place of T_a in Eq. (8). This assumes that the half-hourly or hourly temperature response of RE is the same as that in the 15-day period, the temperature of which was used as the representative mean temperature to determine the empirical coefficients in Eq. (8). In general, the temperature response of RE is determined by using nocturnal eddy covariance CO_2 flux data, and this nocturnal temperature dependence is extrapolated to the daytime (e.g., Goulden et al., 1996; Falge et al., 2002). However, nocturnal eddy covariance surface fluxes calculated by using typical averaging times of about 30 min generally exhibit large scatter because of measurement error by mesoscale motions, since the cospectral gap, which separates turbulence and mesoscale contributions, is commonly located at a time scale of a few minutes or less during the nocturnal period (e.g., Vickers and Mahrt, 2003). Therefore, we extrapolated the daytime temperature dependence of RE to the night-time dependence (e.g., Suyker and Verma, 2001; Gilmanov et al., 2003).

3 Results and discussion

3.1 Variations in parameters among biomes

We examined the relationships between estimated annual NPP and unstressed maximum P_{max} at all sites (Fig. 4a). Increasing NPP was correlated with increasing unstressed maximum P_{max}, regardless of the biome types. Since NPP is estimated by using annual mean temperature or annual precipitation, this result suggests that canopy assimilation capacity, to a large degree, depends critically upon the temperature and water conditions at the measurement sites. The NPP response of the unstressed maximum P_{max} varied among biomes: the unstressed maximum P_{max} in savanna was the most sensitive to NPP, and that in evergreen broad-leaf forest was the least sensitive (Table 2 and Fig. 4a).

We plotted regression lines of initial slope, estimated as a linear functions of P_{max}, for every biome (Fig. 4b). At the plant level, previous studies (e.g., Ehleringer and Björkman, 1977; Ehleringer and Pearcy, 1983) have shown that initial slope is nearly universally the same among unstressed plants. At the canopy level in the current analyses, however, the initial slopes for the seven biomes showed clear seasonal variations: these may result from changes in plant developmental stages, regulated mainly by temperature and water supply. A remarkable point in Fig. 4b is the similarities in the correlation between P_{max} and initial slope for all biomes analyzed. This result prompts one to speculate that the relationship between P_{max} and initial slope is universal regardless of biome type. A similar result has been reported by Owen et al. (2007). It would be interesting to investigate this relationship of initial slope in the nonrectangular hyperbola. However, little information is available on the physiological mechanisms behind the general relationship between initial slope and P_{max}; in the following analyses we therefore used the individual regression lines estimated for each biome (see Table 2).

We examined the relationships between temperature and RE scaled by annual NPP (RE/NPP) for seven biomes (Fig. 4c). The regression curves were extended to

BGD
5, 4001–4034, 2008

both edges of the graph. The sensitivities of RE/NPP to temperature exhibited large variations among biomes. Tundra had the highest rate over the entire temperature range; RE_{ref}, the magnitude of RE/NPP at 10°C, was approximately 0.01 μmol CO_2 s^{-1} $(g\,C\,y^{-1})^{-1}$ (Table 2) – over twice the magnitude of those in the other biomes. Soil carbon density on tundra is higher than in other biomes (Adams et al., 1990), and this carbon richness of the soil could enhance heterotrophic respiration and thence RE/NPP. This simple temperature dependence estimated for every biome was used to represent the diurnal variations in RE at all ecosystem sites.

Before we compared the observed and predicted diurnal variations in NEE, we compared the seasonal changes in P_{max} (example, Fig. 5) and initial slope (example, Fig. 6) computed by the model with those from the observations. Individual points in the graphs are the weekly averaged values of parameters. The seasonal cycle amplitude of P_{max} and initial slope at the Duke Forest site, in an evergreen needle-leaf forest, were larger than at the other sites. The Santarem site, in an evergreen broad-leaf forest, showed large values with small amplitude all year round. The results for the deciduous broad-leaf and mixed forest sites clearly reflected the existence of both growing and non-growing seasons in a year. (The start and end times of the growing season in the mature red pine site are not shown in the figures because of lack of data.) In contrast, variability of P_{max} and initial slope was always appropriate at the evergreen sites. The seasonal courses of the modeled P_{max} and initial slope, and the magnitudes of these two parameters, showed good agreement with those from the observation data. In addition, the model captured well the timing of the start and end of ecosystem productivity. Of course, although the developmental physiology of plants is regulated by both endogenous and external factors (Larcher, 2003), these results seem to favor the explanation that temperature and VPD play primal roles as external factors in determining the seasonal variability of the physiological parameters involved in photosynthesis, and moreover in the seasonality of growth and development of plants.

The proposed model, however, failed to predict the seasonal cycles of P_{max} and initial slope in savanna and some of the grassland sites (not shown). In savanna,

BGD
5, 4001–4034, 2008

analysis of the observation data revealed that the duration of the assimilation period was restricted to a narrow period of about 100 days, and the seasonal patterns of the parameters were very sharp. These processes were less sensitive to changes in temperature and VPD than were those in other biomes. Leuning et al. (2005) have shown that the productivity of the savanna ecosystem is controlled almost exclusively by the amount and timing of rainfall during the wet season. Ma et al. (2007) pointed out similarly that both photosynthesis and respiration processes in savanna depend on the amount of seasonal precipitation. These previous studies suggest that precipitation is the dominant factor controlling ecosystem productivity in savanna under drought conditions. In order to apply this sensitivity of photosynthesis in the savanna to precipitation, however, it is necessary to understand of the relationship between the physiological processes in savanna ecosystems and precipitation. We therefore used an empirical filter in the shape of triangle, with a zero at the two ends of the base and a 1 at the apex. From the given data, filter width was empirically determined as 200 days and the position of the apex was DOY (day of year) 240. This filter was applied to both parameters (P_{max} and initial slope) for all savanna sites, whereas RE was estimated without a filter. The shape of the filter, filter width, and apex position were set artificially in order to reproduce the sharp increase and decrease in ecosystem productivity characteristic of the given savanna data; therefore, these procedures differed among different sites.

Some of the grassland sites also exhibited disagreement between the modeled P_{max} and initial slope and the observed values. This was due to the fact that these grasslands are subject to grazing pressure, or influenced by field management operations such as mowing. Grazing intensity markedly affects above-ground biomass (e.g., Cao et al., 2004) and can thus cause variations in ecosystem productivity. However, grazing intensity and frequency, and types of human field management, are site-specific, and it is difficult to generally characterize the influence of these stresses. Unfortunately, this problem remains to be solved.

Yuan et al. (2007) developed a light-use-efficiency model with information on a normalized difference vegetation index (NDVI); the model was able to predict seasonal

variability in GPP in grassland and savanna biomes. Similarly, Leuning et al. (2005) reasonably estimated seasonal variability in savanna during the wet season by using Moderate Resolution Imaging Spectroradiometer (MODIS) data. These remote-sensing data products respond directly to changes in overall canopy conditions such as leaf area index and canopy structure. For the savanna and disturbed grassland biomes, these data may be useful for further advancement of the proposed model.

3.2 Variations in NEE

Next, to demonstrate the capability of the proposed model, we compared the observed and predicted values of NEE. Variations in half-hourly or hourly NEE were calculated for all sites during the entire periods for which input meteorological data were available (Fig. 7). The figure plots the class-averaged model-predicted NEE for every 0.5 or 1 μmol CO_2 m^{-2} s^{-1} class against the corresponding observed NEE. Despite the fact that this was a very simple model based on empirical regression methods, it showed good performance for half-hourly or hourly variations in NEE over long periods, especially for forest biomes, and the deviations from the one-to-one line were not large. These results imply that the nonrectangular hyperbola with biome-specific seasonality of physiological parameters can be applied to various biomes to predict diurnal variation in NEE. However, at some of the sites, especially in tundra, the model-predicted NEE was overestimated or underestimated when compared with the observed one, although the magnitude of NEE variability was small (between −4 and 2 μmol CO_2 m^{-2} s^{-1}). It should be noted that the eddy covariance CO_2 flux data analyzed include some degree of scatter by random measurement error, which limits the agreement between data and model (Richardson and Hollinger, 2005). Therefore, the discrepancy between the observed and predicted NEE is in part probably due to this uncertainty in measurement.

We examined the diurnal courses of the observed and model-predicted half-hourly NEE at the Atqasuk tundra site (which had exhibited the worst correlation between the observations and the model predictions in Fig. 7) for a selected 6-day period in the mid-

BGD
5, 4001–4034, 2008

dle of July 2004 (Fig. 8). The discrepancies are obvious during the daytime on DOY 191 and 194. Some of the observed half-hourly NEEs have positive values (indicating CO_2 release from the ecosystem) during the daytime. The large disagreement at Atqasuk resulted in part from this variability in the observed data. However, despite the very small fluctuations in NEE (within $\pm 4\,\mu mol\,CO_2\,m^{-2}\,s^{-1}$), Fig. 8 shows that the diurnal variation and the magnitude of the predicted NEE were in reasonable agreement with the observations.

The poor agreement between the observed and predicted NEE at some of grassland sites (Fig. 7) is attributable mainly to the disturbance caused by field management at these sites. However, intermediate hardwood and WLEF sites in mixed forests also exhibited large discrepancies in half-hourly NEE variations. The four mixed-forest sites analyzed were closed to each other (see Table 1), so environmental conditions differed little among the sites. As a consequence, it was difficult to determine regression lines characteristic of the relationship between the physiological parameters and environmental factors at each of these sites. This is a limitation of the proposed empirical-regression-based model. Further studies of mixed forests using data obtained at different sites covering various ranges in temperature, VPD, and precipitation variability are therefore needed to validate the model.

3.3 Nocturnal RE

As mentioned above, the model uses the response of the daytime ecosystem respiration to temperature in order to estimate RE variability between both daytime and nighttime over the entire period. The half-hourly or hourly nocturnal RE variability predicted by the model, being mainly indicated by positive NEE values (Figs. 7 and 8), seems to be adequately close to the observed variability. To demonstrate the ability of the model to predict RE variability, as the typical example we show the seasonal course of monthly averaged nocturnal RE for both the observations and the model at the Howland forest site, in an evergreen needle-leaf forest, in 2004 (Fig. 9). The model captures the seasonal cycle of the nocturnal RE, but the computed amplitudes are somewhat

smaller than those of the observation data. The model slightly overestimates RE in winter and underestimates in summer; the difference between the observations and the model is within approximately 1 μmol CO_2 m^{-2} s^{-1}.

This difference could be, in part, attributed to the simplifying approach of the model. In the interest of constructing the model as simply as possible, RE variability over a year was introduced with a single equation as a function of temperature, regardless of any differences between growing seasons and non-growing seasons. A recent study by Sampson et al. (2007), however, has demonstrated that there is considerable variability in the temperature dependence of soil respiration in association with seasonal differences in photosynthesis. They suggest that the temperature response of soil respiration increases with increasing photosynthetic rate owing to enhanced substrate supply. However, to avoid complexity and obviate the need to obtain additional information on the mechanics of the relationship between RE and photosynthesis rate, the model does not account for the influence of these physiological activities on RE. On the other hand, as shown by the large error bars in Fig. 9, it is also clear that the nocturnal eddy covariance data provide large scatter associated with weak turbulence. This noise is mainly due to flux sampling error, which may, in part, be the cause of the difference between the observed and predicted RE. In view of these problems with both the observation data and the model predictions, we consider that the model estimated diurnal and seasonal variability in RE with moderate accuracy, although it is important to be aware of the abovementioned problems when computing RE variability with the model.

4 Conclusions

We explored a simple approach to predicting diurnal variation in NEE over seven biomes and proposed an empirical model based on the use of a nonrectangular hyperbola and eddy covariance flux data obtained from the AmeriFlux network. Physiological parameters in the nonrectangular hyperbola – P_{max}, initial slope, and RE – clearly

exhibited seasonal variations. We showed that this seasonality in parameters could be adequately expressed as a function of environmental variables – air temperature, VPD, annual mean air temperature, and annual precipitation – at the site. The proposed model successfully predicted the diurnal variability in NEE for various biomes – especially for forest biomes – over the entire yearly observation period, although uncertainties remain in the case of disturbed grassland and savanna biomes. The approach used here would be applicable to other regions. Adjustment of the methodology used in the parameter estimations and subdivision of the biome types would further improve the precision of the model.

Acknowledgements. This study is part of the GOSAT project promoted by the Japan Aerospace Exploration Agency, the National Institute for Environmental Studies, Japan, and the Ministry of the Environment, Japan. We acknowledge Yanhong Tang for useful comments on the manuscript. We also acknowledge NOAA Earth System Research Laboratory and Pennsylvania State University for providing the data. Funding for research at Bartlett and Howland AmeriFlux sites was provided by the Northeastern States Research Cooperative, the US. Department of Energy's Office of Science (BER) through the Northeastern Regional Center of the National Institute for Climatic Change Research and the Terrestrial Carbon Program under Interagency Agreemant No. DE-AI02-00ER63028, with additional support from the USDA Forest Service's Northern Global Change program and Northern Research Station. G. Katul acknowledges support from the US Department of Energy (DOE) through the Office of Biological and Environmental Research (BER) Terrestrial Carbon Processes (TCP) program (Grants No. 10509-0152, DE-FG02-00ER53015, and DE-FG02-95ER62083).

References

Adams, J. M., Faure, H., Faure-Denard, L., McGlade, J. M., and Woodward, F. I.: Increases in terrestrial carbon storage from the last glacial maximum to the present, Nature, 348, 711–714, 1990. 4011

Baldocchi, D. D., Falge, E., Gu, L. H., Olson, R., Hollinger, D., Running, S., Anthoni, P., Bernhofer, C., Davis, K., Evans, R., Fuentes, J., Goldstein, A., Katul, G., Law, B., Lee, X. L., Malhi, Y., Meyers, T., Munger, W., Oechel, W., Paw U, K. T., Pilegaard, K., Schmid, H. P., Valentini,

R., Verma, S., Vesala, T., Wilson, K., and Wofsy, S.: FLUXNET: a new tool to study the temporal and spatial variability of ecosystem-scale carbon dioxide, water vapor and energy flux densities, B. Am. Meteorol. Soc., 82, 2415–2434, 2001. 4003

Bonan, G. B.: A land surface model (LSM version 1.0) for ecological, hydrological, and atmospheric studies: Technical description and user's guide, NCAR Tech. Note NCAR/TN-417+STR, 150 pp., 1996. 4003

Bonan, G. B.: The land surface climatology of the NCAR Land Surface Model coupled to the NCAR Community Climate Model, J. Climate, 11, 1307–1326, 1998. 4003

Cao, G., Tang, Y., Mo, W., Wang, Y., Li, Y., and Zhao, X.: Grazing intensity alters soil respiration in an alpine meadow on the Tibetan plateau, Soil Biol. Biochem., 36, 237–243, 2004. 4012

Dore, S., Hymus, G. J., Johnson, D. P., Hinkle, C. R., Valentini, R., and Drake, B. G.: Cross validation of open-top chamber and eddy covariance measurements of ecosystem CO_2 exchange in a Florida scrub-oak ecosystem, Global Change Biol., 9, 84–95, 2003. 4023

Ehleringer, J. and Björkman, O.: Quantum yield for CO_2 uptake in C_3 and C_4 plants, Plant Physiol., 59, 86–90, 1977. 4010

Ehleringer, J. and Pearcy, R. W.: Variation in quantum yield for CO_2 uptake among C_3 and C_4 plants, Plant Physiol., 73, 555–559, 1983. 4010

Epstein, H. E., Calef, M. P., Walker, M. D., Chapin, F. S., and Starfield, A. M.: Detecting changes in arctic tundra plant communities in response to warming over decadal time scales, Global Change Biol., 10, 1325–1334, 2004. 4023

Eugster, W., Rouse, W. R., Pielke, R. A., McFadden, J. P., Baldocchi, D. D., Kittel, T. G. F., Chapin, F. S., Liston, G. E., Vidale, P. L., Vaganov, E., and Chambers, S.: Land-atmosphere energy exchange in Arctic tundra and boreal forest: available data and feedbacks to climate, Global Change Biol., 6, 84–115, 2000. 4023

Falge, E., Baldocchi, D., Olson, R., Anthoni, P., Aubinet, M., Bernhofer, C., Burba, G., Ceulemans, R., Clement, R., Dolman, H., Granier, A., Gross, P., Grünwald, T., Hollinger, D., Jensen, N. O., Katul, G., Keronen, P., Kowalski, A., Lai, C. T., Law, B. E., Meyers, T., Moncrieff, J., Moors, E., Munger, J. W., Pilegaard, K., Rannik, Ü., Rebmann, C., Suyker, A., Tenhunen, J., Tu, K., Verma, S., Vesala, T., Wilson, K., and Wofsy, S.: Gap filling strategies for defensible annual sums of net ecosystem exchange, Agr. Forest Meteorol., 107, 43–69, 2001. 4008

Falge, E., Baldocchi, D., Tenhunen, J., Aubinet, M., Bakwin, P., Berbigier, P., Bernhofer, C., Burba, G., Clement, R., Davis, K. J., Elbers, J. A., Goldstein, A. H., Grelle, A., Granier, A.,

Guðmundsson, J., Hollinger, D., Kowalski, A. S., Katul, G., Law, B. E., Malhi, Y., Meyers, T., Monson, R. K., Munger, J. W., Oechel, W., Paw U, K. T., Pilegaard, K., Rannik, Ü., Rebmann, C., Suyker, A., Valentini, R., Wilson, K., and Wofsy, S.: Seasonality of ecosystem respiration and gross primary production as derived from FLUXNET measurements, Agr. Forest Meteorol., 113, 53–74, 2002. 4009

Farquhar, G. D., von Caemmerer, S., and Berry, J. A.: A biochemical model of photosynthetic CO_2 assimilation in leaves of C_3 species, Planta, 149, 78–90, 1980. 4003

Fung, I. Y., Tucker, C. J., and Prentice, K. C.: Application of Advanced Very High Resolution Radiometer vegetation index to study atmosphere-biosphere exchange of CO_2, J. Geophys. Res., 92, 2999–3015, 1987. 4002

Gholz, H. L. and Clark, K. L.: Energy exchange across a chronosequence of slash pine forests in Florida, Agr. Forest Meteorol., 112, 87–102, 2002. 4023

Gilmanov, T. G., Verma, S. B., Sims, P. L., Meyers, T. P., Bradford, J. A., Burba, G. G., and Suyker, A. E.: Gross primary production and light response parameters of four Southern Plains ecosystems estimated using long-term CO_2-flux tower measurements, Global Biogeochem. Cy., 17, 1071, doi:10.1029/2002GB002023, 2003. 4005, 4007, 4009

Gilmanov, T. G., Tieszen, L. L., Wylie, B. K., Flanagan, L. B., Frank, A. B., Haferkamp, M. R., Meyers, T. P., and Morgan, J. A.: Integration of CO_2 flux and remotely-sensed data for primary production and ecosystem respiration analyses in the Northern Great Plains: potential for quantitative spatial extrapolation, Global Ecol. Biogeogr., 14, 271–292, 2005. 4023

Gilmanov, T. G., Soussana, J. F., Aires, L., Ammann, C., Balzarola, M., Barcza, Z., Bernhofer, C., Campbell, C. L., Cernusca, A., Cescatti, A., Clifton-Brown, J., Dirks, B. O. M., Dore, S., Eugster, W., Fuhrer, J., Gimeno, C., Gruenwald, T., Haszpra, L., Hensen, A., Ibrom, A., Jacobs, A. F. G., Jones, M. B., Lanigan, G., Laurila, T., Lohila, A., Manca, G., Marcolla, B., Nagy, Z., Pilegaard, K., Pinter, K., Pio, C., Raschi, A., Rogiers, N., Sanz, M. J., Stefani, P., Sutton, M., Tuba, Z., Valentini, R., and Williams, M. L.: Partitioning European grassland net ecosystem CO_2 exchange into gross primary productivity and ecosystem respiration using light response function analysis, Agric. Ecosyst. Environ., 121, 93–120, 2007. 4008

Goulden, M. L., Munger, J. W., Fan, S. M., Daube, B. C., and Wofsy, S. C.: Measurements of carbon sequestration by long-term eddy covariance: methods and a critical evaluation of accuracy, Global Change Biol., 2, 169–182, 1996. 4009, 4023

Gu, L., Meyers, T., Pallardy, S. G., Hanson, P. J., Yang, B., Heuer, M., Hosman, K. P., Riggs, J. S., Sluss, D., and Wullschleger, S. D.: Direct and indirect effects of atmospheric condi-

tions and soil moisture on surface energy partitioning revealed by a prolonged drought at a temperate forest site, J. Geophys. Res., 111, D16102, doi:10.1029/2006JD007161, 2006. 4023

Gutschick, V. P.: Joining leaf photosynthesis models and canopy photon-transport models, in: Photon-Vegetation Interaction: Applications in Optical Remote Sensing and Plant Ecology, edited by: Myneni, R. B. and Ross, J., 505–535, Springer-Verlag, 1991. 4005

Hargrove, W. W., Hoffman, F. M., and Law, B. E.: New analysis reveals representativeness of AmeriFlux network, Eos Trans. AGU, 84, 529, 2003. 4004

Hirata, R., Saigusa, N., Yamamoto, S., Ohtani, Y., Ide, R., Asanuma, J., Gamo, M., Hirano, T., Kondo, H., Kosugi, Y., Li, S., Nakai, Y., Takagi, K., Tani, M., and Wang, H.: Spatial distribution of carbon balance in forest ecosystems across East Asia, Agr. Forest Meteorol., 148, 761–775, 2008. 4005

Hollinger, D. Y., Aber, J., Dail, B., Davidson, E. A., Goltz, S. M., Hughes, H., Leclerc, M., Lee, J. T., Richrdson, A. D., Rodrigues, C., Scott, N. A., Varier, D., and Walsh, J.: Spatial and temporal variability in forest-atmospheric CO_2 exchange, Global Change Biol., 10, 1689–1706, 2004. 4023

Ito, A. and Oikawa, T.: A simulation model of the carbon cycle in land ecosystems (Sim-CYCLE): a description based on dry-matter production theory and plot-scale validation, Ecol. Model., 151, 143–176, 2002. 4006

Jenkins, J. P., Richardson, A. D., Braswell, B. H., Ollinger, S. V., Hollinger, D. Y., and Smith, M. L.: Refining light-use efficiency calculations for a deciduous forest canopy using simultaneous tower-based carbon flux and radiometric measurements, Agr. Forest Meteorol., 143, 64–79, 2007. 4023

Johnson, I. R. and Thornley, J. H. M.: A model of instantaneous and daily canopy photosynthesis, J. Theor. Biol., 107, 531–545, 1984. 4005

Katul, G., Leuning, R., and Oren, R.: Relationship between plant hydraulic and biochemical properties derived from a steady-state coupled water and carbon transport model, Plant Cell Environ., 26, 339–350, 2003. 4023

Katul, G. G., Hsieh, C., Bowling, D., Clark, K., Shurpali, N., Turnipseed, A., Albertson, J., Tu, K., Hollinger, D., Evans, B., Offerle, B., Anderson, D., Ellsworth, D., Vogel, C., and Oren, R.: Spatial variability of turbulent fluxes in the roughness sublayer of an even-aged pine forest, Bound.-Lay. Meteorol., 93, 1–28, 1999. 4023

Larcher, W.: Physiological Plant Ecology, Ecophysiology and Stress Physiology of Functional

Groups, Springer-Verlag, 513 pp., 2003. 4011
LeMone, M. A., Grossman, R. L., McMillen, R. T., Liou, K. N., Ou, S. C., McKeen, S., Angevine, W., Ikeda, K., and Chen, F.: Cases-97: Late-morning warming and moistening of the convective boundary layer over the Walnut River Watershed, Bound.-Lay. Meteorol., 104, 1–52, 2002. 4023
Leuning, R.: Modeling stomatal behavior and photosynthesis of *Eucalyptus grandis*, Aust. J. Plant Physiol., 17, 159–175, 1990. 4006
Leuning, R., Cleugh, H. A., Zegelin, S. J., and Hughes, D.: Carbon and water fluxes over a temperate *Eucalyptus* forest and a tropical wet/dry savanna in Australia: measurements and comparison with MODIS remote sensing estimates, Agr. Forest Meteorol., 129, 151–173, 2005. 4012, 4013
Lieth, H.: Modeling the primary productivity of the world, in: Primary Productivity of the Biosphere, edited by: Lieth, H. and Whittaker, R. H., 237–263, Springer-Verlag, 1975. 4007
Lloyd, J. and Taylor, J. A.: On the temperature dependence of soil respiration, Funct. Ecol., 8, 315–323, 1994. 4008
Ma, S., Baldocchi, D. D., Xu, L., and Hehn, T.: Inter-annual variability in carbon dioxide exchange of an oak/grass savanna and open grassland in California, Agr. Forest Meteorol., 147, 157–171, 2007. 4012, 4023
Martens, C. S., Shay, T. J., Mendlovitz, H. P., Matross, D. M., Saleska, S. R., Wofsy, S. C., Woodward, W. S., Menton, M. C., De Moura, J. M. S., Crill, P. M., De Moraes, O. L. L., and Lima, R. L.: Radon fluxes in tropical forest ecosystems of Brazilian Amazonia: night-time CO_2 net ecosystem exchange derived from radon and eddy covariance methods, Global Change Biol., 10, 618–629, 2004. 4023
McMillan, A. M. S., Winston, G. C., and Goulden, M. L.: Age-dependent response of boreal forest to temperature and rainfall variability, Global Change Biol., 14, 1904–1916, 2008. 4023
Monteith, J. L.: Solar radiation and productivity in tropical ecosystems, J. Appl. Ecol., 9, 747–766, 1972. 4003
Nemry, B., Francois, L., Gérard, J. C., Bondeau, A., Heimann, M., and the participants of the Potsdam NPP Model Intercomparison: Comparing global models of terrestrial net primary productivity (NPP): analysis of the seasonal atmospheric CO_2 signal, Global Change Biol., 5, 65–76, 1999. 4002
Owen, K. E., Tenhunen, J., Reichstein, M., Wang, Q., Falge, E., Geyer, R., Xiao, X., Stoy, P., Ammann, C., Arain, A., Aubinet, M., Bernhofer, C., Chojnicki, B. H., Granier, A., Gruenwald,

T., Hadley, J., Heinesch, B., Hollinger, D., Knohl, A., Kutsch, W., Lohila, A., Meyers, T., Moors, E., Moureau, C., Pilegaard, K., Saigusa, N., Verma, S., Vesala, T., and Vogel, C.: Linking flux network measurements to continental scale simulations: ecosystem carbon dioxide exchange capacity under non-water-stressed conditions, Global Change Biol., 13, 734–760, 2007. 4007, 4010

Peat, W. E.: Relationships between photosynthesis and light intensity in the tomato, Ann. Bot. London, 34, 319–328, 1970. 4005

Potter, C. S., Randerson, J. T., Field, C. B., Matson, P. A., Vitousek, P. M., Moonet, H. A., and Klooster, S. A.: Terrestrial ecosystem production: a process model based on global satellite and surface data, Global Biogeochem. Cy., 7, 811–841, 1993. 4003

Rabinowitch, E. I.: Photosynthesis and Related Processes, Interscience Publishers, 608 pp., 1951. 4005

Raich, J. W., Rastetter, E. B., Melillo, J. M., Kicklighter, D. W., Grace, A. L., Moore III, B., and Vörösmarty, C. J.: Potential net primary productivity in South America: application of a global model, Econ. Appl., 1, 399–429, 1991. 4006

Randerson, J. T., Thompson, M. V., Conway, T. J., Fung, I. Y., and Field, C. B.: The contribution of terrestrial sources and sinks to trends in the seasonal cycle of atmospheric carbon dioxide, Global Biogeochem. Cy., 11, 535–560, 1997. 4003

Reichstein, M., Tenhunen, J. D., Roupsard, O., Ourcival, J.-. M., Rambal, S., Miglietta, F., Peressotti, A., Pecchiari, M., Tirone, G., and Valentini, R.: Severe drought effects on ecosystem CO_2 and H_2O fluxes at three Mediterranean evergreen sites: revision of current hypotheses?, Global Change Biol., 8, 999–1017, 2002. 4008

Reichstein, M., Falge, E., Baldocchi, D., Papale, D., Aubinet, M., Berbigier, P., Bernhofer, C., Buchmann, N., Gilmanov, T., Granier, A., Grünwald, T., Havránková, K., Ilvesniemi, H., Janous, D., Knohl, A., Laurila, T., Lohila, A., Loustau, D., Matteucci, G., Meyers, T., Miglietta, F., Ourcival, J. M., Pumpanen, J., Rambal, S., Rotenberg, E., Sanz, M., Tenhunen, J., Seufert, G., Vaccari, F., Vesala, T., Yakir, D., and Valentini, R.: On the separation of net ecosystem exchange into assimilation and ecosystem respiration: review and improved algorithm, Global Change Biol., 11, 1424–1439, 2005. 4008

Richardson, A. D. and Hollinger, D. Y.: Statistical modeling of ecosystem respiration using eddy covariance data: Maximum likelihood parameter estimation, and Monte Carlo simulation of model and parameter uncertainty, applied to three simple models, Agr. Forest Meteorol., 131, 191–208, 2005. 4013

Ruimy, A., Dedieu, G., and Saugier, B.: TURC: a diagnostic model of continental gross primary productivity and net primary productivity, Global Biogeochem. Cy., 10, 269–285, 1996. 4003
Sampson, D. A., Janssens, I. A., Curiel Yuste, J., and Ceulemans, R.: Basal rates of soil respiration are correlated with photosynthesis in a mixed temperate forest, Global Change Biol., 13, 2008–2017, 2007. 4008, 4015
Schwarz, P. A., Law, B. E., Williams, M., Irvine, J., Kurpius, M., and Moore, D.: Climatic versus biotic constraints on carbon and water fluxes in seasonally drought-affected ponderosa pine ecosystems, Global Biogeochem. Cy., 18, GB4007, doi:10.1029/2004GB002234, 2004. 4023
Scott, R. L., Jenerette, G. D., Potts, D. L., and Huxman, T. E.: The effect of drought on the water and carbon dioxide exchange of a woody-plant-encroached semiarid grassland, Agr. Forest Meteorol., in review, 2008. 4023
Sellers, P. J., Mintz, Y., Sub, Y. C., and Dalcher, A.: A simple biosphere model (SiB) for use within general circulation models, J. Atmos. Sci., 43, 305–331, 1986. 4003
Suyker, A. E. and Verma, S. B.: Year-round observations of the net ecosystem exchange of carbon dioxide in a native tallgrass prairie, Global Change Biol., 7, 279–289, 2001. 4009
Thornley, J. H. M.: Instantaneous Canopy Photosynthesis: Analytical Expressions for Sun and Shade Leaves Based on Exponential Light Decay Down the Canopy and an Acclimated Non-rectangular Hyperbola for Leaf Photosynthesis, Ann. Bot., 81, 451–458, 2002. 4003
Vickers, D. and Mahrt, L.: The cospectral gap and turbulent flux calculations, J. Atmos. Ocean. Tech., 20, 660–672, 2003. 4009
Wang, C. K., Bond-Lambery, B., and Gower, S. T.: Carbon distribution of a well- and poorly-drained black spruce fire chronosequence, Global Change Biol., 9, 1066–1079, 2003. 4023
Xu, L. and Baldocchi, D. D.: Seasonal variation in carbon dioxide exchange over a Mediterranean annual grassland in California, Agr. Forest Meteorol., 123, 79–96, 2004. 4008, 4023
Yi, C. X., Davis, K. J., Berger, B. W., and Bakwin, P. S.: Long-term observations of the dynamics of the continental planetary boundary layer, J. Atmos. Sci., 58, 1288–1299, 2001. 4023
Yuan, W., Liu, S., Zhou, G., Zhou, G., Tieszen, L. L., Baldocchi, D., Bernhofer, C., Gholz, H., Goldstein, A. H., Goulden, M. L., Hollinger, D. Y., Hu, Y., Law, B. E., Stoy, P. C., Vesala, T., and Wofsy, S. C.: Deriving a light use efficiency model from eddy covariance flux data for predicting daily gross primary production across biomes, Agr. Forest Meteorol., 143, 189–207, 2007. 4012

Table 1. List of AmeriFlux eddy covariance measurement sites analyzed in this study.

Site, country	Year	Latitude, longitude	Reference
Evergreen needle leaf forest (ENF)			
UCI-1930 burn site, Canada	2002–2004	55.91° N, 98.53° W	Wang et al. (2003)
UCI-1850 burn site, Canada	2002–2004	55.88° N, 98.48° W	McMillan et al. (2008)
Duke Forest loblolly pine, USA	2002–2004	35.98° N, 79.09° W	Katul et al. (1999)
Howland forest, USA	2002–2004	45.20° N, 68.74° W	Hollinger et al. (2004)
Metolius, USA	2004–2005	44.45° N, 121.56° W	Schwarz et al. (2004)
Slashpine-Donaldson, USA	2002–2004	29.76° N, 82.16° W	Gholz and Clark (2002)
Evergreen broad leaf forest (EBF)			
Santarem-Km67-Primary Forest, Brazil	2002–2004	2.86° S, 54.96° W	Martens et al. (2004)
Florida-Kennedy Space Center, USA	2004–2006	28.61° N, 80.67° W	Dore et al. (2003)
Deciduous broad leaf forest (DBF)			
Duke Forest hardwoods, USA	2003–2005	35.97° N, 79.10° W	Katul et al. (2003)
Harvard Forest EMS Tower, USA	2001–2003	42.54° N, 72.17° W	Goulden et al. (1996)
Missouri Ozark Site, USA	2005–2006	38.74° N, 92.20° W	Gu et al. (2006)
Bartlett Experimental Forest, USA	2004–2005	44.07° N, 71.29° W	Jenkins et al. (2007)
Mixed forest (MF)			
Intermediate hardwood, USA	2003	46.73° N, 91.23° W	——
Mature red pine, USA	2003–2005	46.74° N, 91.17° W	——
Mixed young jack pine, USA	2004	46.65° N, 91.09° W	——
Park Falls/WLEF, USA	1997, 1999	45.95° N, 90.27° W	Yi et al. (2001)
Grassland (GRS)			
Duke Forest open field, USA	2002–2004	35.97° N, 79.09° W	Katul et al. (2003)
Fort Peck, USA	2003–2005	48.31° N, 105.10° W	——
Brookings, USA	2005–2006	44.35° N, 96.84° W	Gilmanov et al. (2005)
Vaira Ranch, USA	2002–2004	38.41° N, 120.95° W	Xu and Baldocchi (2004); Ma et al. (2007)
Walnut River Watershed, USA	2002–2004	37.52° N, 96.86° W	LeMone et al. (2002)
Savanna (SVN)			
Santa Rita Mesquite, USA	2004–2006	31.82° N, 110.87° W	Scott et al. (2008)
Audubon Research Ranch, USA	2004–2006	31.59° N, 110.51° W	——
Tundra (TND)			
Atqasuk, USA	2004–2006	70.47° N, 157.41° W	——
Barrow, USA	2000–2002	71.32° N, 156.63° W	Eugster et al. (2000)
Ivotuk, USA	2004–2006	68.49° N, 155.75° W	Epstein et al. (2004)

BGD

5, 4001–4034, 2008

Table 2. List of ecosystem-specific parameter values.

Types	Terms	Eq. (3)				Eq. (4)		Eq. (6)		Eq. (7)		Eq. (8)	
		AMT	T_{max}	T_{min}	T_{opt}	a_{FV}	b_{FV}	a_{PM}	b_{PM}	a_{Ini}	b_{Ini}	RE_{ref}	E_0
	Units	˚C	˚C	˚C	˚C	–	kPa	–	–	(μmol photon m^{-2} s^{-1})$^{-1}$	μmol CO_2 (μmol photon)$^{-1}$	μmol CO_2 s^{-1} (g C y^{-1})$^{-1}$	–
ENF		>15 (≤15)	45 (40)	5 (0)	25 (20)	−0.5	0	14.63	0.0015	0.00075	0.0059	0.0053	190.0
EBF		–	45	5	30	−1.0	0	34.7	0.00024	0.0014	−0.0058	0.0015	399.3
DBF		>13 (≤13)	40 (40)	12 (10)	25 (22)	−0.5	0	13.41	0.0018	0.00078	0.008	0.0031	241.0
MF		–	40	5	18	−0.6	0	16.4	0.0012	0.0012	0.0003	0.0028	305.1
GRS		>12 (≤12)	45 (40)	5 (0)	27 (20)	−0.45	0	7.43	0.002	0.00082	0.0059	0.0025	252.0
SVN		–	40	10	25	−0.65	1	2.87	0.0058	0.0009	0.0028	0.00066	588.1
TND		–	25	−3	12	−0.4	0	3.8	0.0031	0.0011	0.0048	0.0105	82.0

BGD
5, 4001–4034, 2008

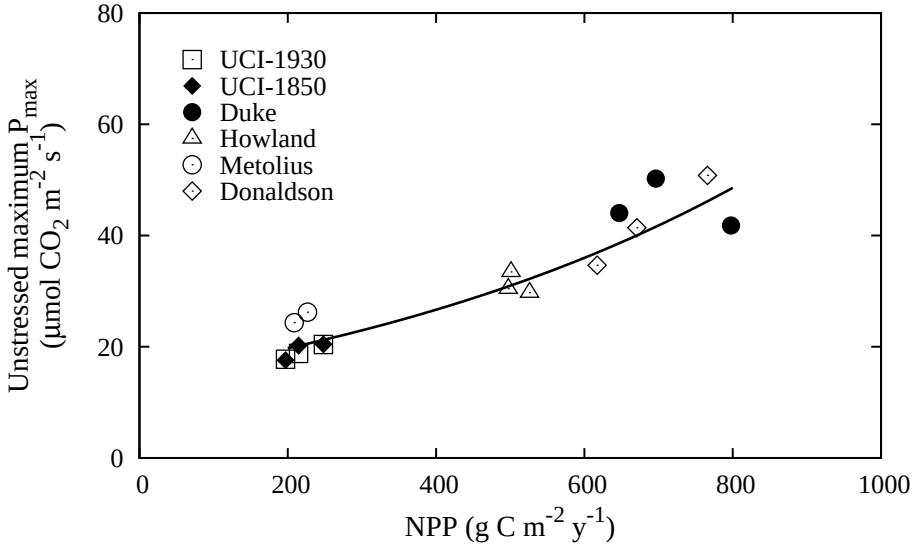

Fig. 1. Relationship between annual NPP and unstressed maximum P_{max} in evergreen needle-leaf forests. Sites are indicated as follows: open squares, UCI-1930 burn; solid diamonds, UCI-1850 burn; solid circles, Duke Forest loblolly pine; open triangles, Howland forest; open circles, Metolius; and open diamonds Slashpine-Donaldson, for each year. Solid line is the regression curve.

BGD
5, 4001–4034, 2008

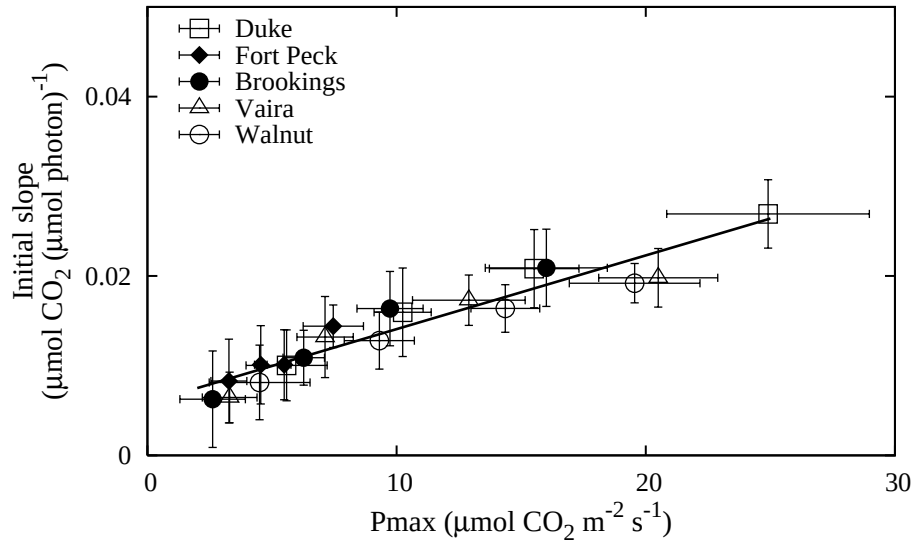

Fig. 2. Relationship between bin-averaged P_{max} and initial slope α in grassland. Sites are indicated as follows: open squares, Duke forest open field; solid diamonds, Fort Peck; solid circles, Brookings; open triangles, Vaira Ranch; and open circles Walnut River Watershed. Solid line is the regression curve, and error bars represent standard deviation from the mean.

BGD
5, 4001–4034, 2008

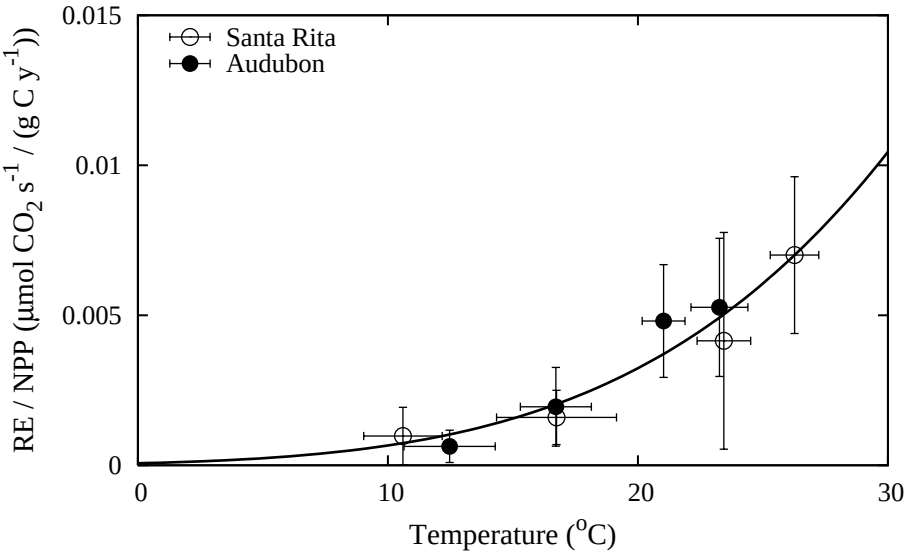

Fig. 3. Relationship between bin-averaged temperature and ecosystem respiration scaled by annual NPP in savannas. Open circles represent Santa Mesquite site and solid circles Audubon Research Ranch site. Solid line is the regression curve, and error bars represent standard deviation from the mean.

BGD
5, 4001–4034, 2008

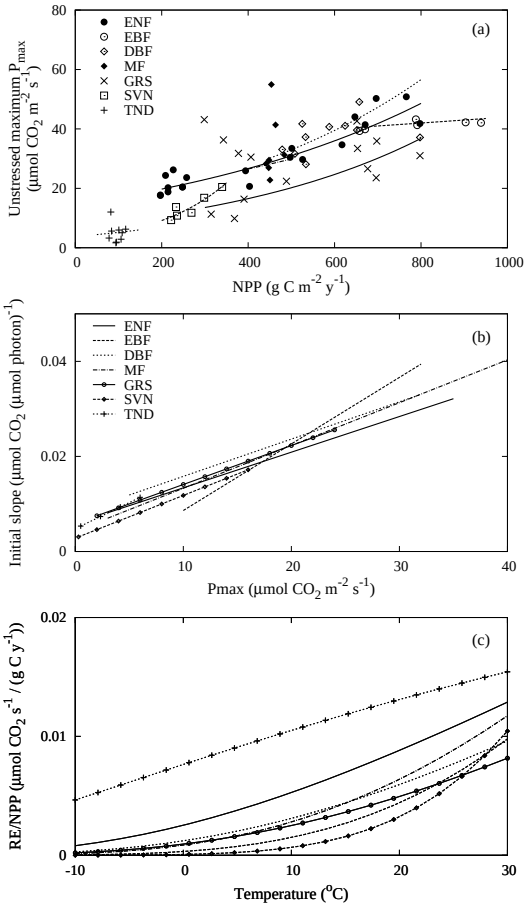

Fig. 4.

BGD
5, 4001–4034, 2008

Fig. 4. Distributions of three parameters for seven biomes: **(a)** Same as Fig. 1, but for all biomes analyzed. Solid circles and solid regression curve represent ENF, open circles with dashed curve EBF, open diamonds with dotted curve DBF, solid diamonds with dashed-dotted curve MF, crosses with solid curve GRS, open square with dashed curve SVN, and pluses with dotted curve TND. **(b)** Relationships between P_{max} and initial slope, and **(c)** between temperature and RE scaled by NPP. Solid line represent ENF, dashed line EBF, dotted line DBF, dashed-dotted line MF, open circles with solid line GRS, open diamonds with dashed line SVN, and pluses with dotted line TND.

BGD
5, 4001–4034, 2008

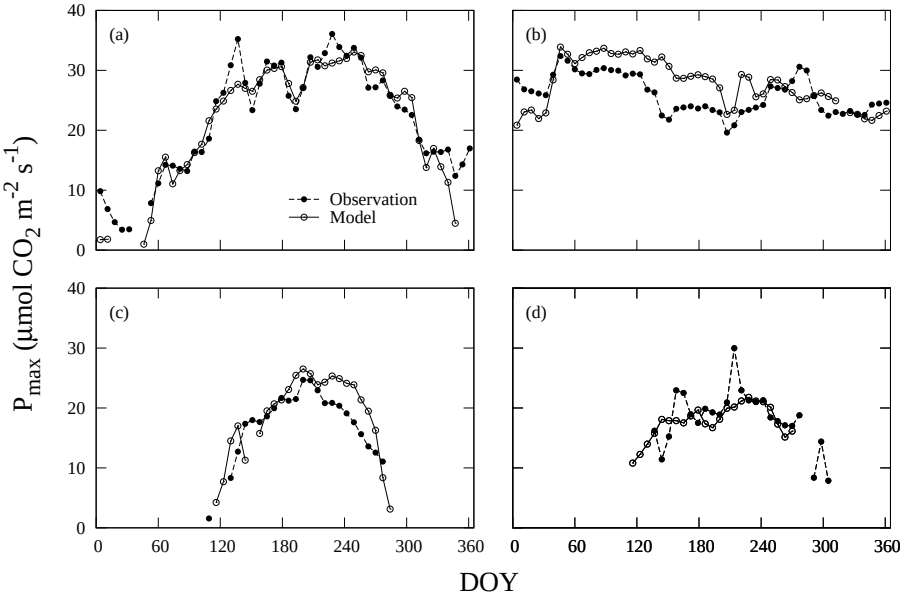

Fig. 5. Seasonal course of weekly averaged P_{max} at **(a)** Duke Forest site, ENF; **(b)** Santarem site, EBF; **(c)** Bartlett site, DBF; and **(d)** Mature red pine site, MF in 2004. Dashed line with closed circles represents P_{max} estimated from the observed data, and solid line with open circles is P_{max} predicted by using the proposed model. DOY=day of year.

BGD
5, 4001–4034, 2008

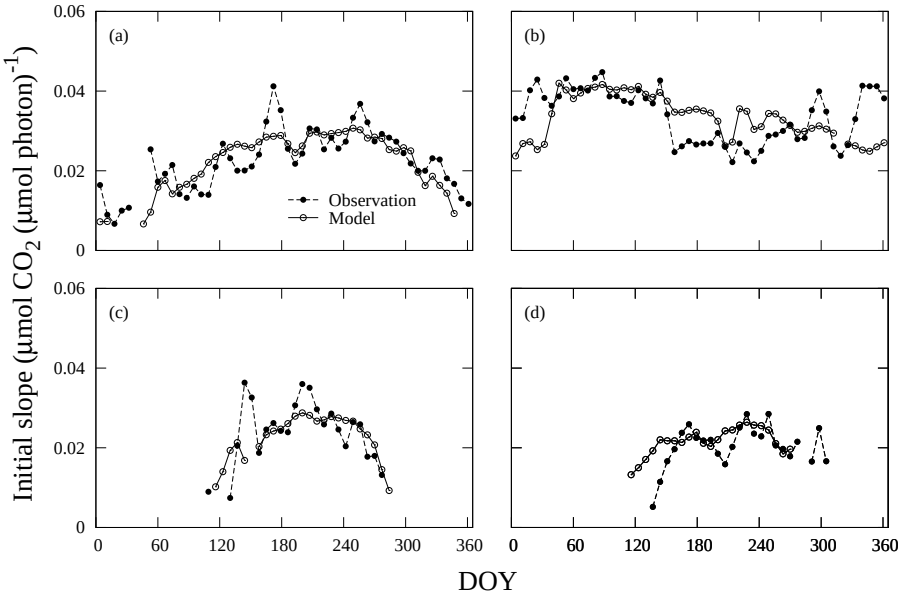

Fig. 6. Same as Fig. 5, but for initial slope.

BGD
5, 4001–4034, 2008

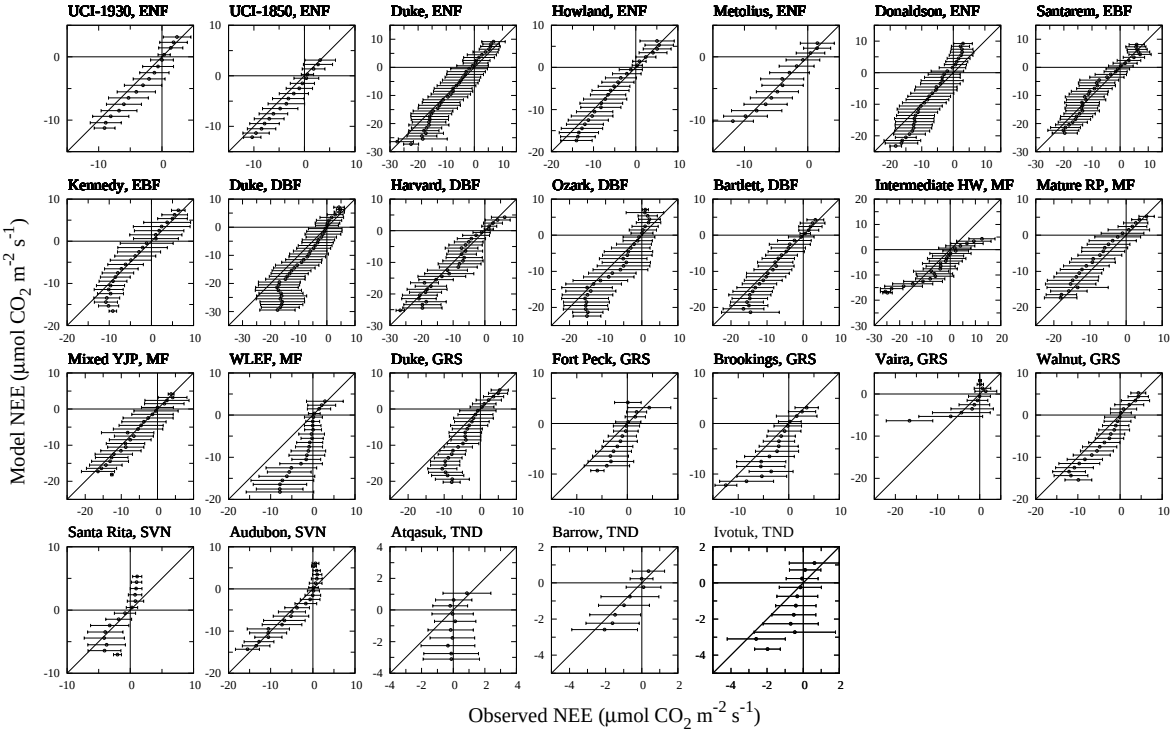

Fig. 7. Class-averaged half-hourly or hourly variations in predicted and observed NEE for all sites. Open circles represent averages, and error bars are standard deviation from the mean.

BGD
5, 4001–4034, 2008

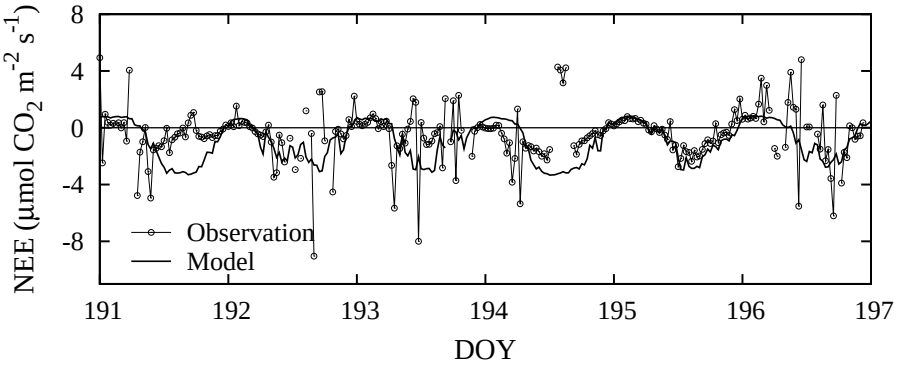

Fig. 8. Comparison of observed and predicted half-hourly NEE at Atqasuk during the period DOY 191 to 196 in 2004. Solid line with open circles represent the observation data, and solid line without circles is the model data.

BGD
5, 4001–4034, 2008

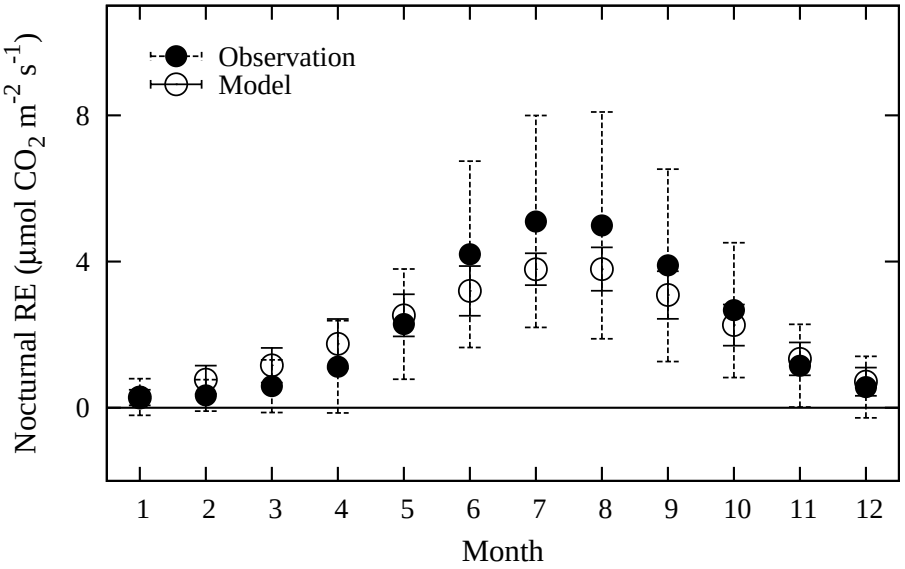

Fig. 9. Seasonal course of monthly averaged nocturnal RE at the Howland ENF site in 2004. Dashed line with closed circles represents the observation data, and solid line with open circles is the model data. Error bars represent the standard deviation from the mean.

BGD
5, 4001–4034, 2008